

Photogenerated charge transfer in Dion-Jacobson type layered perovskite based on Naphthalene diimide

Simon Nussbaum,^a Etienne Socie,^b George C. Fish,^b Nicolas J. Diercks,^a Hannes Hempel,^c Dennis Friedrich,^d Jacques-E. Moser,^b Jun-Ho Yum,^{*a} Kevin Sivula^{*a}

^aLaboratory for Molecular Engineering of Optoelectronic Nanomaterials, Institute of Chemical Sciences and Engineering (ISIC), École Polytechnique Fédérale de Lausanne (EPFL), 1015 Lausanne, Switzerland.

E-mail: junho.yum@epfl.ch, kevin.sivula@epfl.ch

^bPhotochemical Dynamics Group, Institute of Chemical Sciences and Engineering (ISIC), École Polytechnique Fédérale de Lausanne (EPFL), 1015 Lausanne, Switzerland.

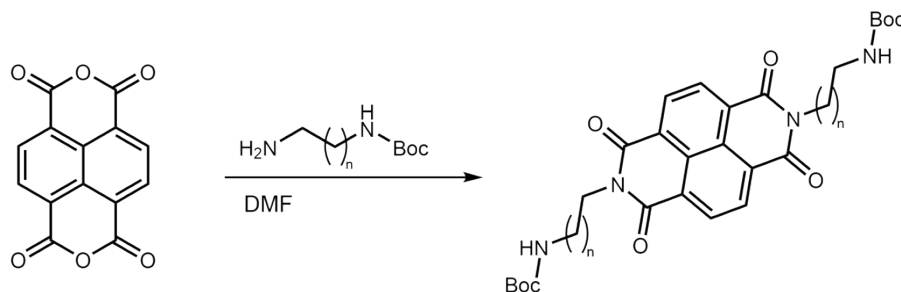
^cDepartment of Structure and Dynamics of Energy Materials, Helmholtz Zentrum Berlin für Materialien und Energie, Hahn-Meitner-Platz 1, 140109 Berlin, Germany.

^dInstitute for Solar Fuels, Helmholtz Zentrum Berlin für Materialien und Energie, Hahn-Meitner-Platz 1, 140109 Berlin, Germany.

Materials and Experimental

Naphthalenedianhydride and NBoc-1,6-diaminohexane were obtained from Fluorochem, NBoc-1,4-diaminobutane was purchased from ABCR. Perovskite precursor solutions were prepared with Lead (II) iodine 99.9999 % from TCI. Methylammonium Iodine was purchased from GreatCell.

Synthesis of the spacer cation



Scheme S1 Synthesis of N-Boc protected NDI-dH

NDI-dH-Boc was synthesized according to previously reported procedure:

5g of naphthalene dianhydride was mixed with NBoc-1,6-diaminohexane in a two-neck flask. After establishing an Argon atmosphere, The reaction mixture was dissolved in 80 ml of N,N-dimethylformamide (DMF) and heated up to 90 °C under continuous stirring. After 12 hours, the reaction mixture was concentrated and redissolved in (dichloromethane) DCM. Residue DMF was removed by 3x extraction with Water. The organic phase was collected and the pure product was obtained in 91 % yield after silica gel chromatography using DCM:ethylacetate as evolving eluent. The product was further purified by recrystallisation from isopropanol:DCM mixture.

^1H NMR (400 MHz, $\text{CDCl}_3\text{-d}$) δ 8.75 (s, 4H), 4.53 (s, 2H), 4.23 – 4.14 (m, 4H), 3.10 (q, $J = 6.5$ Hz, 4H), 1.74 (q, $J = 7.6$ Hz, 4H), 1.55 – 1.37 (m, 4H), 1.43 (m, 26H).

^{13}C NMR (101 MHz, $\text{CDCl}_3\text{-d}$) δ 162.98, 156.13, 121.10, 126.80, 40.90, 30.06, 28.56, 28.08, 26.79, 26.54

HRMS (ESI-QTOF) m/z : $[\text{M} + \text{Na}^+]$: Calcd for $\text{C}_{36}\text{H}_{48}\text{N}_4\text{NaO}_8^+$ 687.3364; Found 687.3380.

Elemental analysis: Anal. Calcd for $\text{C}_{36}\text{H}_{48}\text{N}_4\text{O}_8$: C, 65.04; H, 7.28; N, 8.43. Found: C, 65.07; H, 7.31; N, 8.44.

NDI-dB-Boc

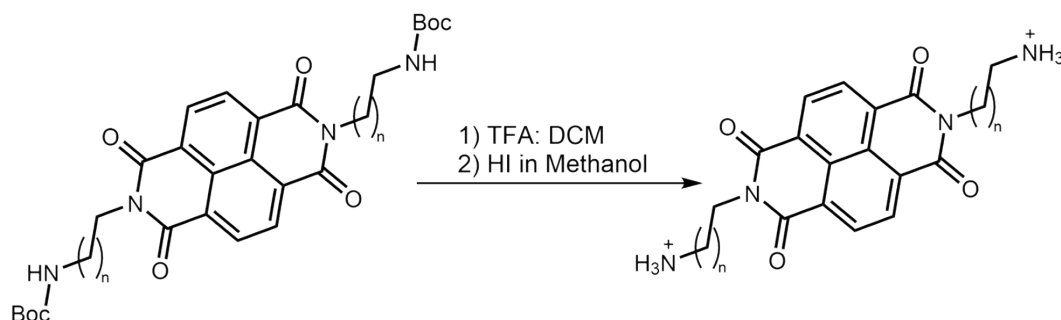
NDI-dB -Boc was synthesized as NDI-dH-Boc

^1H NMR (400 MHz, $\text{CDCl}_3\text{-d}$) δ 8.75 (s, 4H), 4.61 (s, 2H), 4.21 (t, $J = 7.4$ Hz, 4H), 3.20 (q, $J = 6.7$ Hz, 4H), 1.85-1.73 (m, 4H), 1.63 (d, $J = 8.0$ Hz, 4H), 1.42 (s, 18 H).

^{13}C NMR (101 MHz, $\text{CDCl}_3\text{-d}$) δ 162.96, 156.09, 131.14, 126.84, 126.74, 116.78, 40.58, 28.55, 27.77, 25.52

Elemental analysis: Anal. Calcd for $\text{C}_{32}\text{H}_{40}\text{N}_4\text{O}_8$: C, 63.14; H, 6.62; N, 9.20. Found: C, 62.94; H, 6.60; N, 9.06.

Salt formation



Scheme S2 Deprotection and ammonium salt formation of NDI-dH

The NBoc protected NDI-dH was deprotected by dissolving NDI-dH-Boc in 15% TFA:DCM solution. After evaporation the solvent and the excess of TFA, the crude solid was redissolved in methanol. After cooling the solution to 0 °C, 3 eqv. of hydroiodic acid was added. The mixture was stirred for 1 hours. The precipitate was collected by centrifugation and washed with diethyl ether until no yellow liquid could be removed.

^1H NMR (400 MHz, DMSO-d_6) δ 8.67 (s, 4H), 7.61 (br, 6H), 4.11 – 4.02 (m, 4H), 2.80 (t, $J = 7.5$ Hz, 4H), 1.67 (t, $J = 7.4$ Hz, 4H), 1.55 (d, $J = 7.5$ Hz, 4H), 1.38 (td, $J = 8.7, 8.0, 4.2$ Hz, 8H).

^{13}C NMR (101 MHz, DMSO- d_6): 162.61, 130.42, 126.28, 126.28, 38.77, 27.26, 26.90, 26.04, 25.49

HRMS (ESI/QTOF) m/z : $[\text{M}]^+$ Calcd for $\text{C}_{26}\text{H}_{34}\text{N}_4\text{O}_4^{+2}$ 233.1285; Found 233.1296.

NDI-dB

^1H NMR (400 MHz, DMSO- d_6) δ 8.70 (s, 4H), 7.61 (br, 6H), 4.10 (t, $J = 6.9$ Hz, 4H), 2.85 (d, $J = 7.8$ Hz, 4H), 1.73 (q, $J = 7.4$ Hz, 4H), 1.62 (q, $J = 7.3, 6.7$ Hz, 4H)

^{13}C NMR (101 MHz, DMSO) δ 163.23, 131.01, 126.81, 126.67, 39.16, 25.22, 25.09.

HRMS (ESI/QTOF) m/z : $[\text{M}]^+$ Calcd for $\text{C}_{22}\text{H}_{26}\text{N}_4\text{O}_4^{+2}$ 205.0972; Found 205.0977.

Thin-film formation for optical spectroscopy

$n = 1-5$ films were synthesized by spin-coating the precursor solution containing 0.2 M PbI_2 and stoichiometric amount of NDI-dH and methylammonium iodine in DMSO solution at 2000 rpm for 30 seconds on glass substrate. The films were subsequently annealed at 180 °C for 10 minutes.

UV-vis absorption and Transient Absorption spectroscopy

UV-visible light absorption measurements were carried out with a UV-3600 Shimadzu spectrometer. Ultrafast transient absorption (TA) measurements were conducted using a fs chirped-pulse amplified (CPA) Ti:sapphire laser (Clark-MXR, CPA2001). A part of the laser output (778 nm, 1 kHz repetition rate) was frequency-doubled in a 0.5 mm-thick BBO crystal and chopped to generate the pump pulse ($\lambda_{\text{pump}} = 389$ nm, 500 Hz repetition rate). The remaining part of the laser output was focused onto a CaF_2 crystal to produce a white light continuum probe spanning from 400 to 780 nm. The white light is attenuated, and its beam cross section is reduced to ensure homogeneity within the probe area. The probe beam was split before the sample; the signal and the reference were sent into two spectrographs (Spectra Pro 2150i, Princeton Instruments) and detected shot-to-shot using CCD cameras (Hamamatsu S070300906). The dynamics were obtained using a digitally controlled delay stage (PI) in the pump path. The time resolution of the experiment was calculated to be 300 fs using the cross-correlation of the pump and probe beam on a reference glass sample.

To extract the lifetimes displayed in Table S2, we performed a global analysis of the dynamic traces of the bleaching peak. A tri-exponential decay function was used to fit the data from 0.20 ps to 1200 ps leaving the amplitudes and lifetimes free and setting y_0 to 0.^[1]

XRD and GIWAXS

Thin film X-ray diffraction (XRD) measurements were taken in the Bragg–Brentano geometry using nonmonochromatic Cu K α 1 radiation on a Bruker D8 Vario instrument equipped with a LynxEYE XE detector. GIWAXS measurements conducted under ambient conditions using a Bruker Vario D8 TXS with a Eiger 2D detector. An X-ray source (1.5406 Å) at an incidence angle (α) of 2 ° was used. GIWAXS images were processed using the python packages pygix and pyFAI.^[2,3]

fp-TRMC

TRMC measurements were performed by mounting the samples in a microwave cavity cell and placing within a setup similar to the one described elsewhere.^[4] A voltage controlled oscillator (SiversIMA VO3262X) generated the microwaves (X-band region, 8.4–8.7 GHz). During the measurements, a change in the microwave power ($\Delta P/P$) reflected by the cavity upon sample excitation by 3 ns (full-width at half-maximum) pulses of a wavelength tunable optical parametric oscillator (OPO) coupled to a diode-pumped Q-switched Nd:YAG laser at a wavelength of 420 nm (50 Hz repetition rate) was monitored and correlated to the photoinduced change in the conductance of the sample, ΔG , given by

$$\Delta G = -\frac{1 \Delta P}{K P}$$

where K is the sensitivity factor derived from the frequency response of the resonant cavity using an analytical impedance model that considered both the cavity geometry and the substrate and thin film properties. Further details on the TRMC system and data analysis can be found elsewhere.^[5]

$$K = \frac{2Q \left(1 \pm \frac{1}{\sqrt{R_0}} \right)}{\pi f_0 \epsilon_0 \epsilon_r L \beta}$$

Where L is the length of the cavity, β is the ratio of the two remaining cavity dimensions. ϵ_0 and ϵ_r are the vacuum permittivity and relative permittivity that is averaged over the whole cavity, respectively. f_0 is the resonant frequency of the cavity, R_0 the reflectivity of the cavity in resonance, and Q the quality factor of the cavity.

For (BA)₂PbI₄ and (NDI-dH)PbI₄ samples a K-factor of 45'000 was assumed.

Optical-Pump Terahertz-Probe (OPTP) spectroscopy

OPTP was used to measure photoconductivity transients and the initial sum of electron mobility and hole mobility as previously reported^[6] with a time resolution of ~150 fs. To this end, terahertz pulses were generated by optical rectification of 800 nm laser pulses in a ZnTe crystal. After these terahertz pulses have been transmitted through the sample, their electric field E was measured by optoelectronic sampling in a second ZnTe crystal. Additional laser pulses with a length of ~150 fs, a wavelength of 400 nm, and a repetition rate of 150 kHz were used to photo-generate a sheet carrier concentration Δn_s of $2.2 \times 10^{13} \text{cm}^{-2}$ per pulse in the sample. This photoexcitation reduced the transmitted by THz field by ΔE , from which the sheet photoconductivity

$\Delta\sigma_s$ can be obtained by the so-called thin-film approximation:

$$\frac{\Delta\sigma_s}{\sigma_s} = \frac{4\pi e \Delta n_s}{c \epsilon_0 n_{sub}^2}$$

c is the speed of light, ϵ_0 permittivity of vacuum, n_{sub} is the refractive index of the quartz glass substrate at terahertz frequencies of ~2, and e is the elementary charge. The photoconductivity transient is measured by mechanically delaying the pump pulses with respect to the terahertz pulses. The sum mobility is μ_Σ can be obtained from the peak value of the photoconductivity transient and the sheet carrier concentration Δn_s known from the excitation conditions.

SCLC Device fabrication and measurement

Electron-only devices were fabricated based on a Glass/FTO/TiO₂/Perovskite/PCBM/silver architecture. The FTO substrates were cleaned for 30 minutes in the ultrasonic sonicator in acetone, soap-water (Hellmanex) solution, water and Isopropanol. The clean substrates were plasma cleaned for at least 10 minutes before sample deposition. TiO₂ layer was deposited by spin-coating a Titanium isopropoxide solution in ethanol:HCl on the FTO glass substrate according to the conditions reported.^[7,8] The isopropoxide solution was spun-coated at 5000 rpm for 40 s. The films were then thermally annealed, following a ramped annealing step to 500 °C (dwell 45 min)

For optimized perovskite thin-films $\langle n \rangle = 5$, the precursor solution was spun-coated on the FTO/TiO₂ at 2000 rpm for 30 seconds and subsequently annealed at 220 °C. The PCBM electron transport layer was coated according to previous reports:^[9] 10 mg of PCBM dissolved in 1 ml of chlorobenzene was spun-coated at 3000 rpm for 30 seconds and subsequent annealed at 100 °C for 10 minutes.

The thickness of the thin films was initially determined with a Bruker Dektak XT profilometer. Thickness of selected samples were further determined by cross-section SEM to confirm the validity of the determined film thickness.

Electrochemical Impedance spectroscopy (EIS)

The relative permittivity of the thin films was estimated based on the capacitance measured by impedance spectrometry. The capacitance was determined using the impedance.py python package.^[10] For this, a perovskite films was spun-coated on FTO substrate and sandwiched with a gold electrode (0.16 cm²). Based on the determined geometric capacitance (C), assuming a plate capacitor geometry, ϵ is calculated using the device thickness, d and area, A:^[11]

$$\epsilon = \frac{Cd}{A\epsilon_0}$$

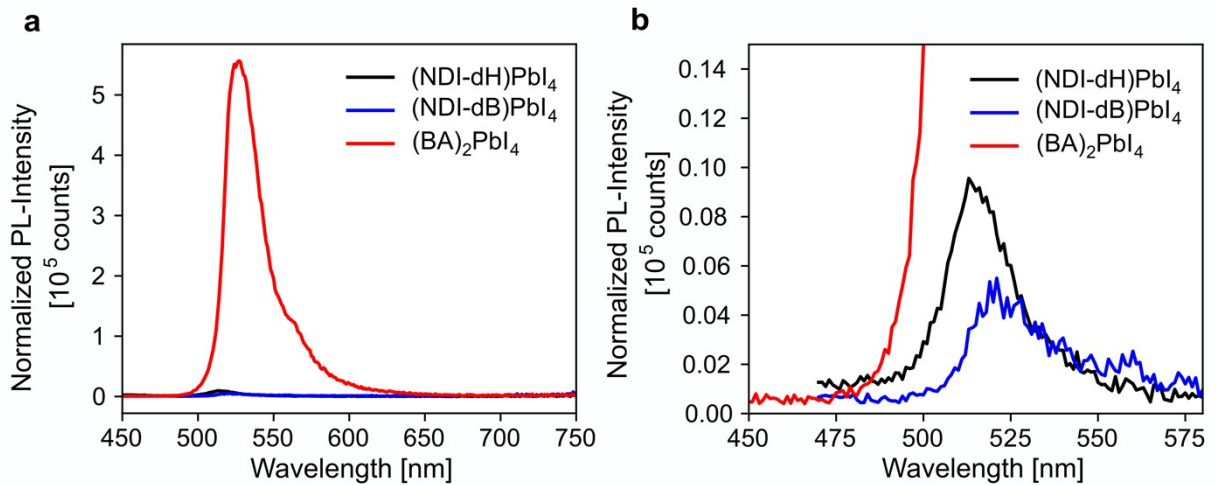


Figure S1 a) PL intensity normalized with respect to the absorption and b) zoomed in PL intensity of (NDI-dH)PbI₄, (NDI-dB)PbI₄, and (BA)₂PbI₄.

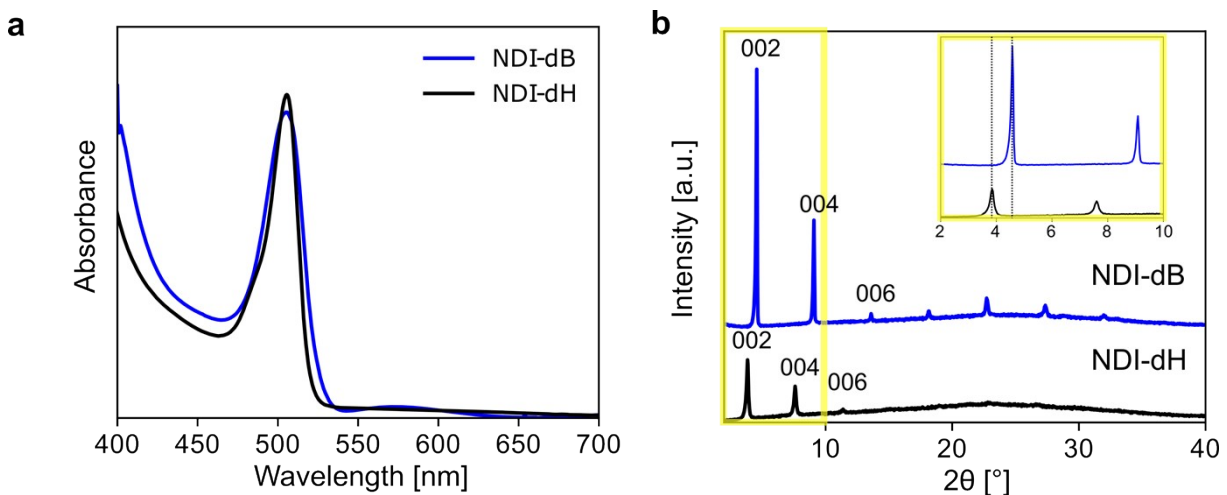


Figure S2 a) UV-vis absorbance and b) XRD of NDI-dH and NDI-dB based (n = 1) layered perovskite thin-films.

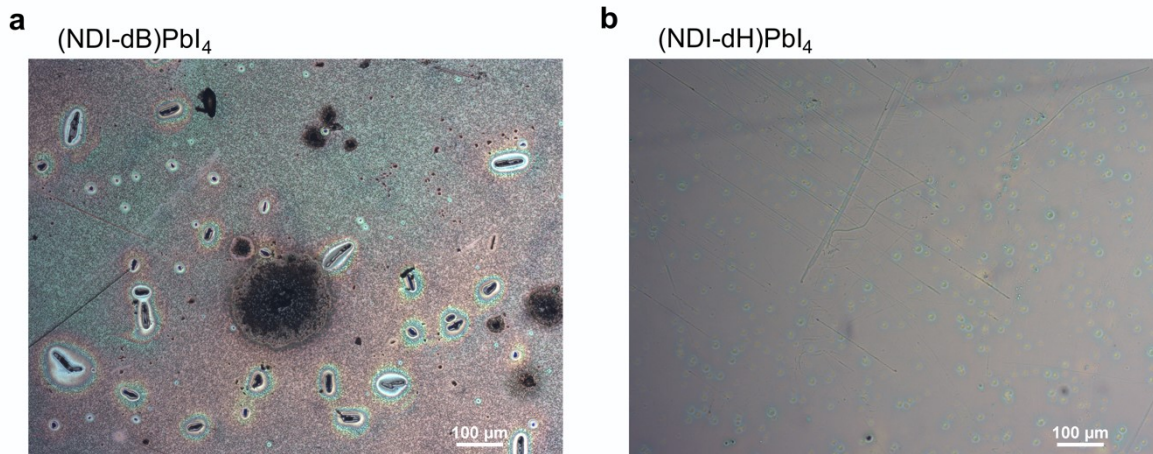


Figure S3 Optical microscope images of a) NDI-dH and b) NDI-dB based ($n = 1$) layered perovskite thin-films solution processed onto glass substrates.

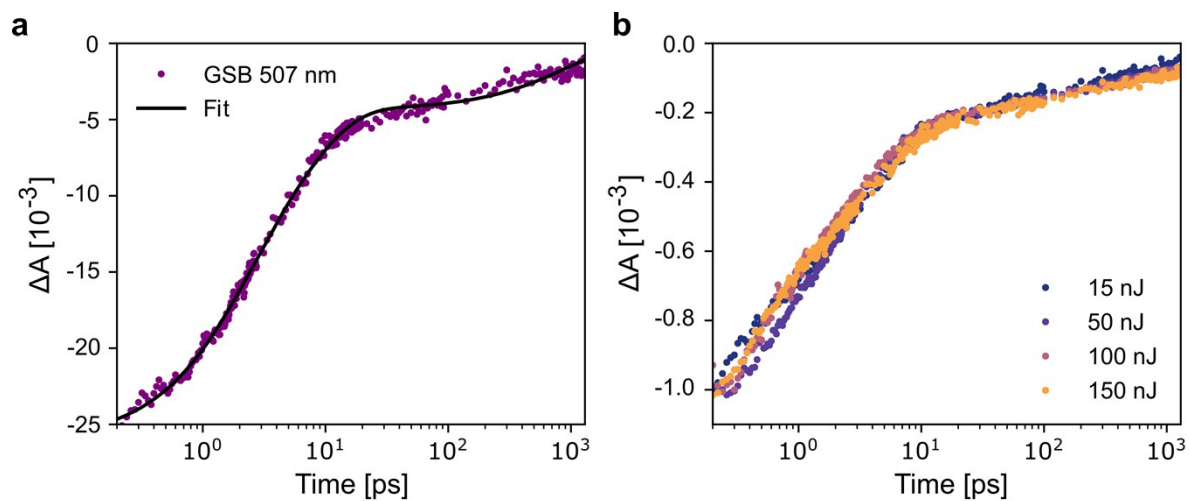


Figure S4 a) Ground state bleach (GSB) dynamics at 507 nm for (NDI-dH)PbI₄ films and b) GSB at 507 nm at different photon flux.

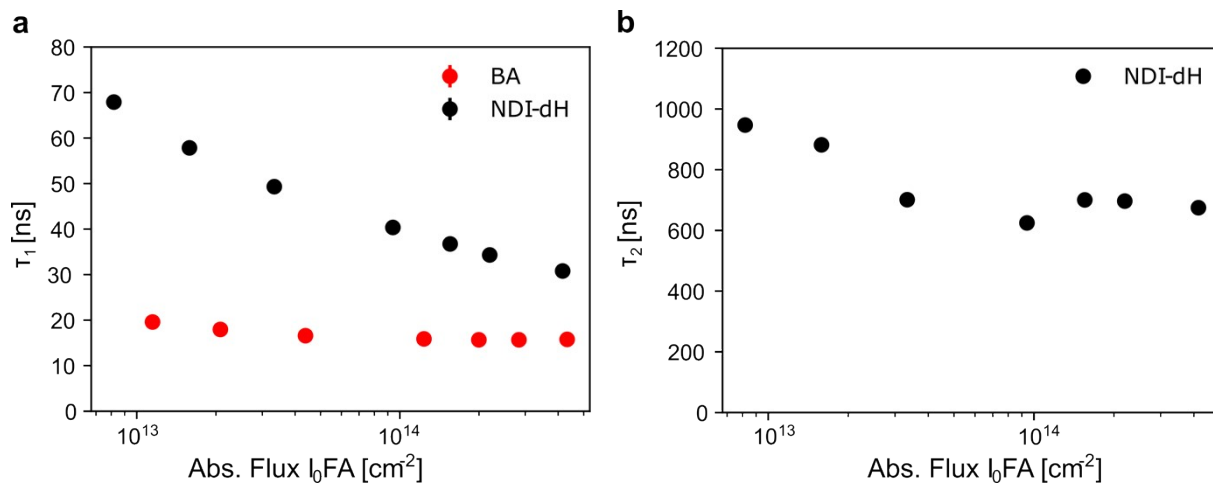


Figure S5 Decay constant of a) τ_1 and b) of τ_2 (only (NDI-dH) PbI_4) of the TRMC transient at different Absorbed photon flux for (BA) $_2PbI_4$ and (NDI-dH) $_2PbI_4$.

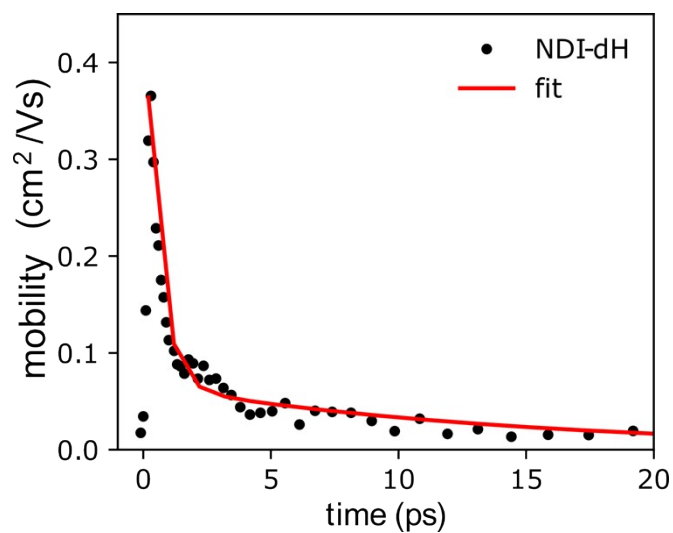


Figure S6 Intrinsic carrier mobility extracted from time-resolved terahertz spectroscopy signals measured for (NDI-dH) PbI_4 excited at 400 nm (photon flux $10 \mu Jcm^{-2}$).

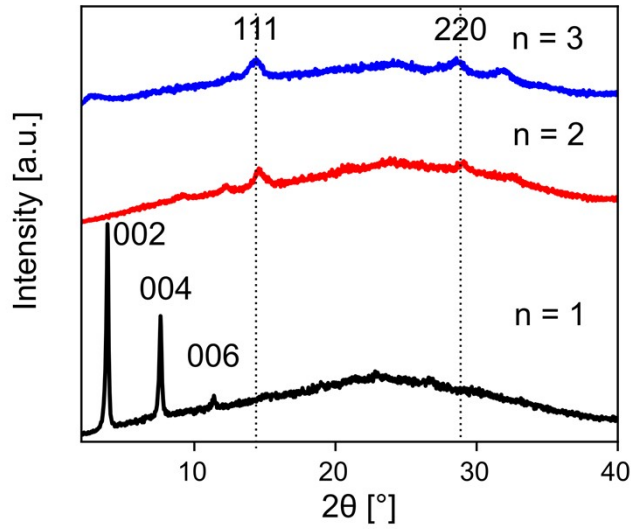


Figure S7 Thin-film XRD of thin-films $n = 1 - 3$ films.

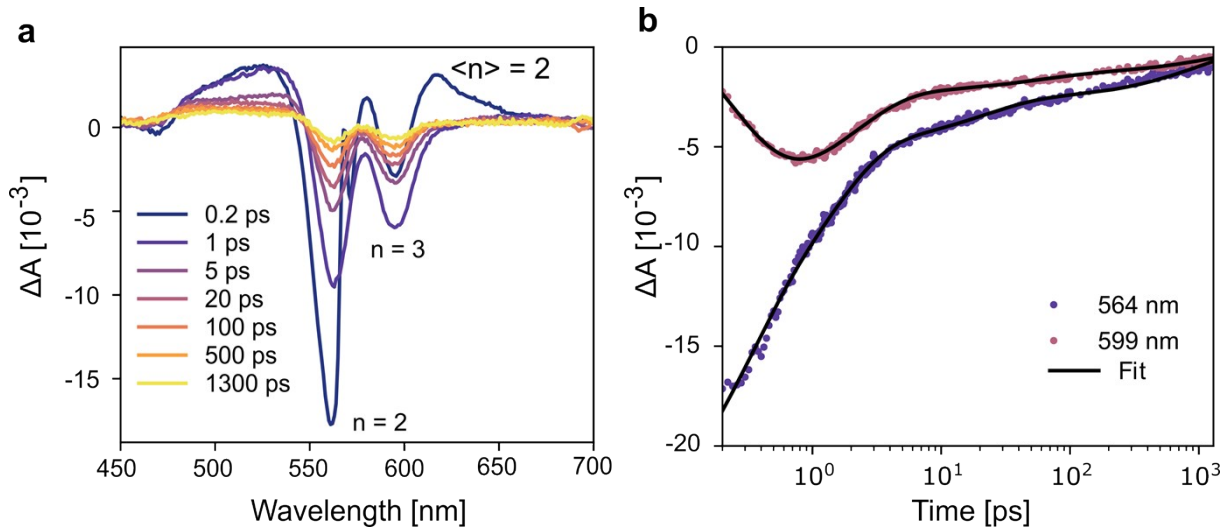


Figure S8 a) TAS of $\langle n \rangle = 2$ film and b) GSB decay and fit of the $n = 2$ and $n = 3$ phase.

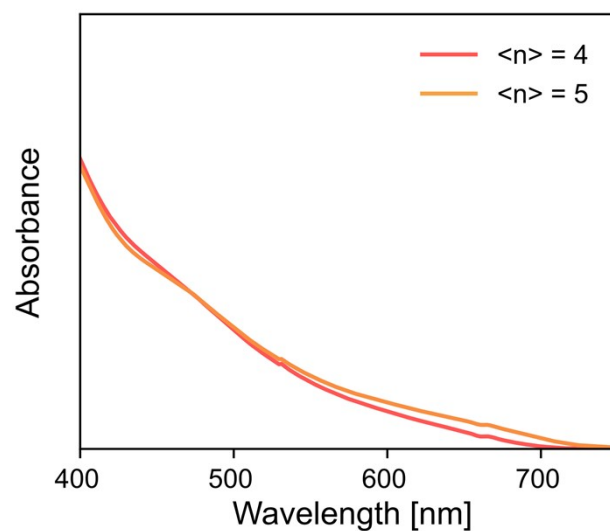


Figure S9 UV-vis absorbance of un-optimized $\langle n \rangle = 4$ and $\langle n \rangle = 5$ films.

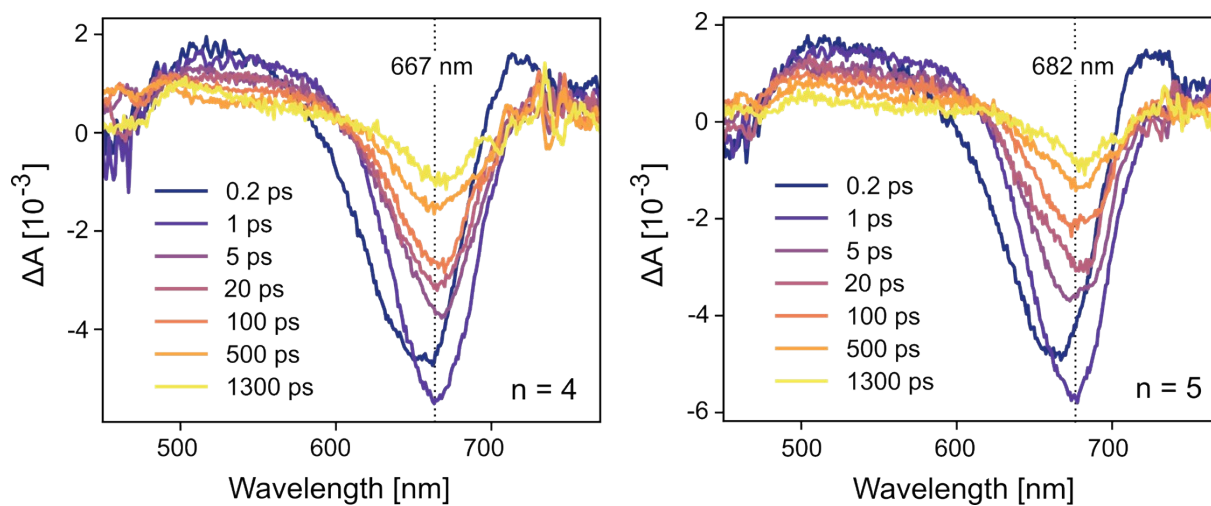


Figure S10 TAS of a) $n = 4$ and b) $n = 5$ film.

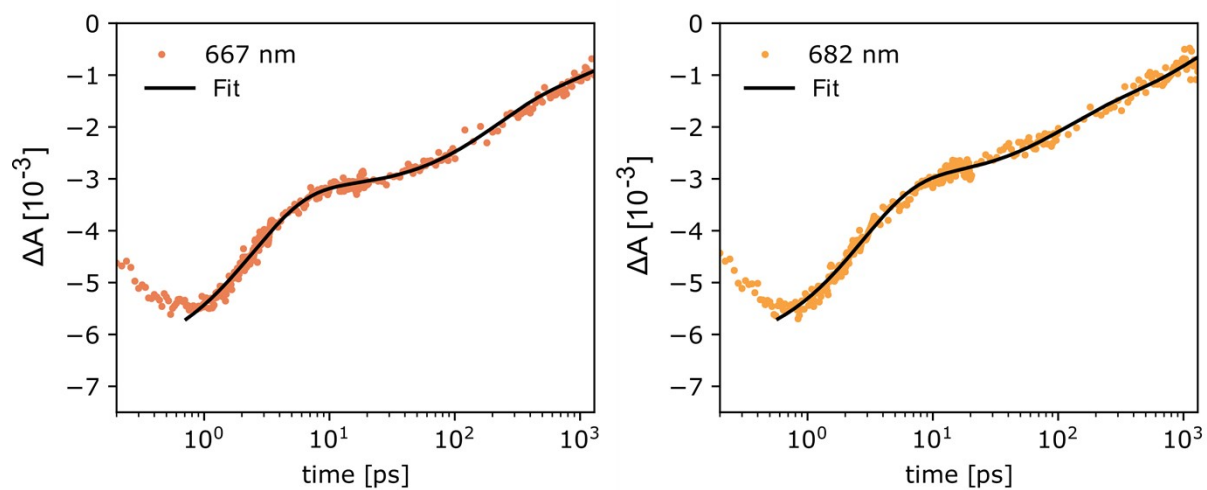


Figure S11 Ground state decay fit for $n = 4$ and $n = 5$ films.

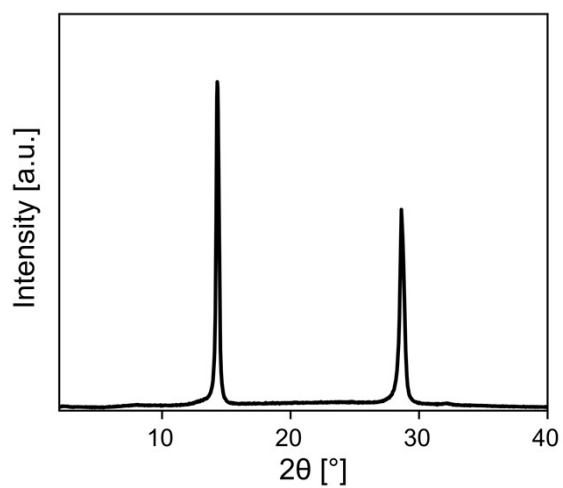


Figure S12 XRD of NDI-dH $\langle n \rangle = 5$ films.

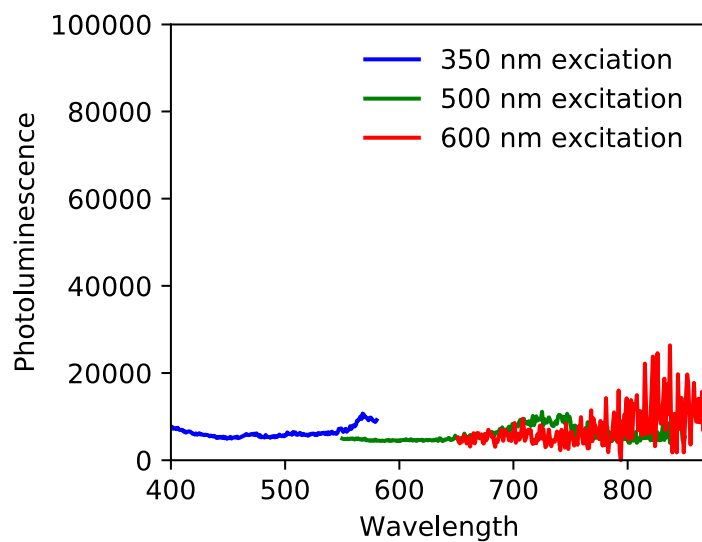


Figure S13 PL of optimized NDI-dH $\langle n \rangle = 5$ films excited at 350 and 600 nm.

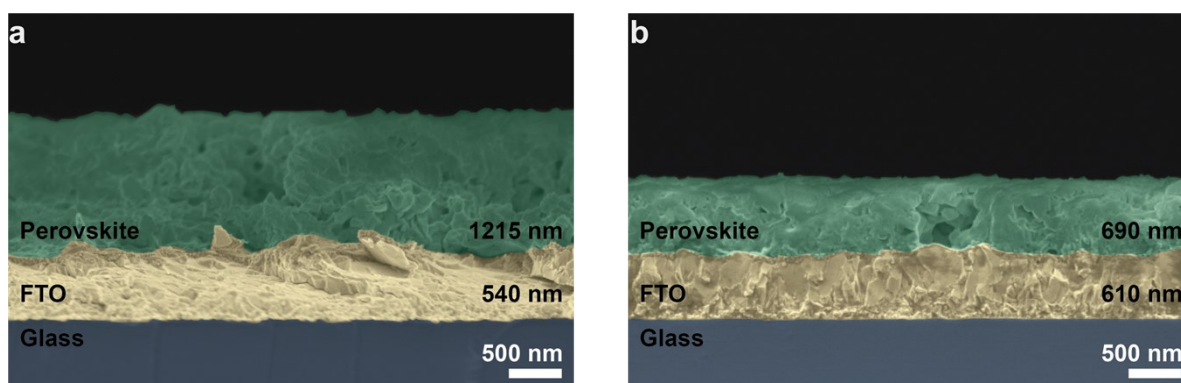


Figure S14 Cross-sectional SEM images of SCLC devices.

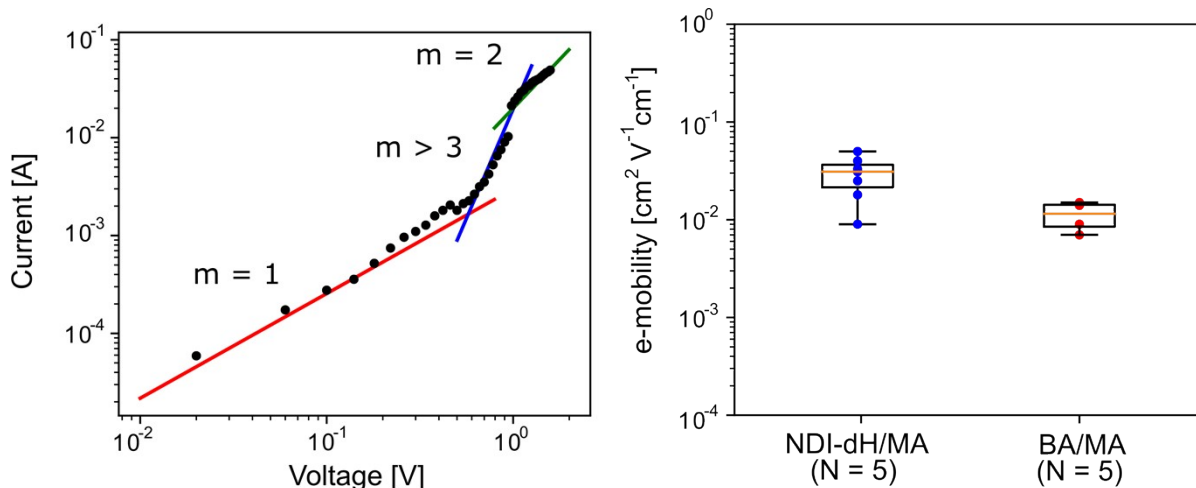


Figure S15 Electron-only mobility obtained from SCLC of BA based ($\langle n \rangle = 5$) films showing Trap-filling region ($m > 3$) and b) comparison of obtained electron mobility for BA and NDI-dH based thin-films.

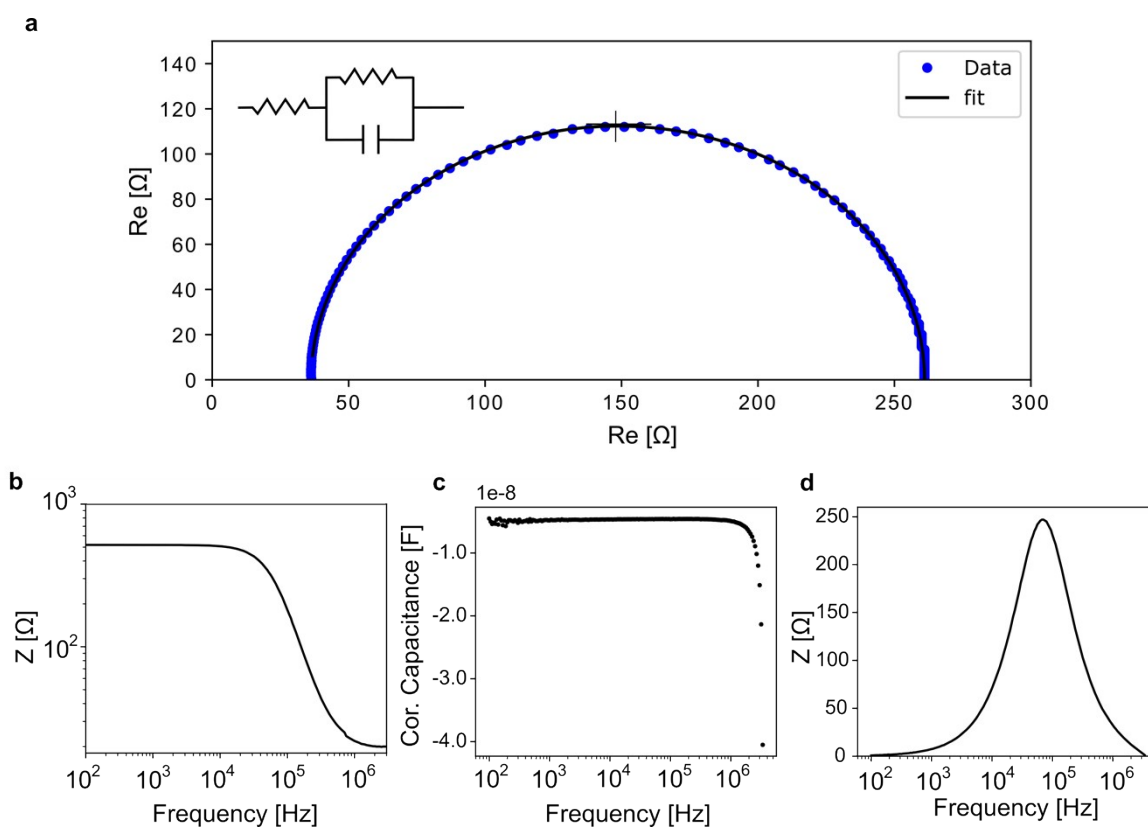


Figure S16 Obtained Impedance spectrum of NDI-dH based perovskite ($\langle n \rangle = 5$). For the measurement the NDI-dH film was spun-coated on FTO and gold electrodes (0.16 cm^2) were evaporated on top. The capacitance was fitted using the python impedancy.py package. The capacitance was calculated based on the imaginary and real value part of the impedance.

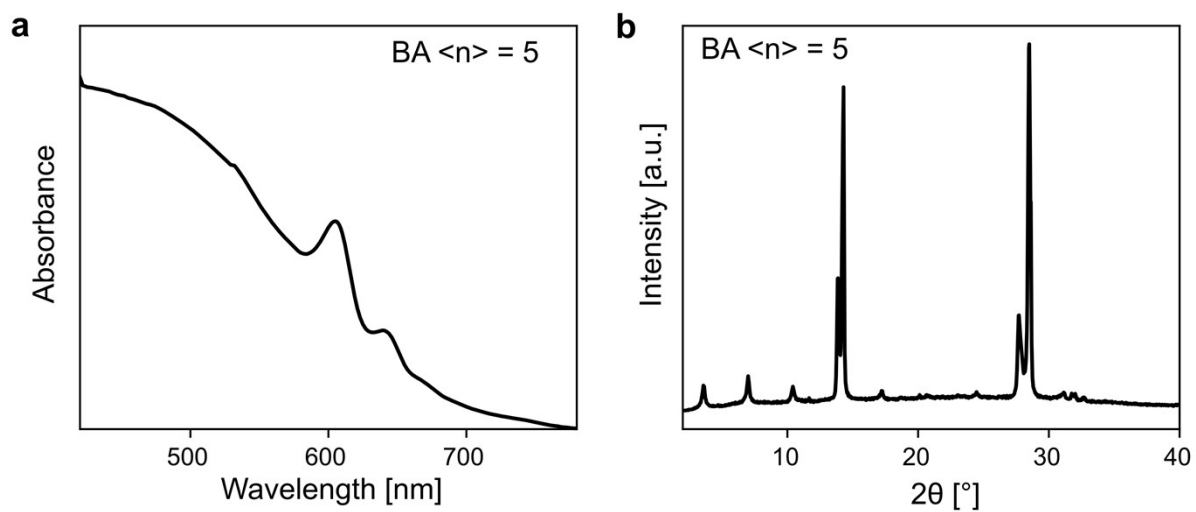


Figure S17 XRD of Butylammonium (BA) based ($\langle n \rangle = 5$) perovskite film.

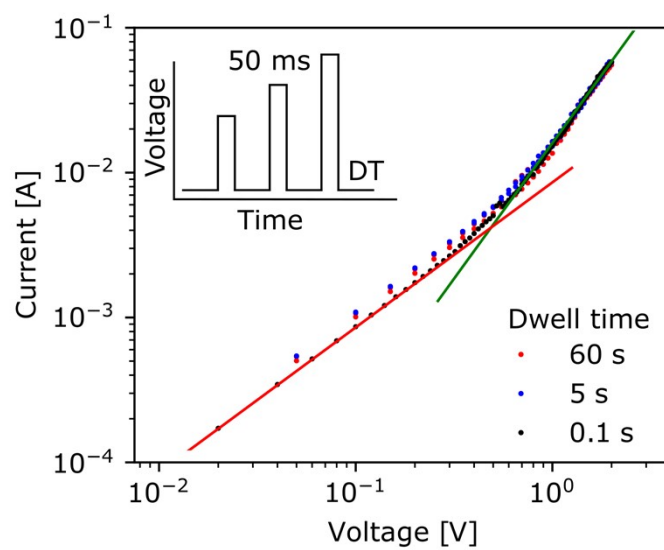


Figure S18 pulsed SCLC with 50 ms voltage pulse with various dwell time.

Table S1 Fit parameters of bi-exponential decay of the OPTP transient ($X^2 = 0.0147$).

	A_1 [%]	τ_1 [ps]	A_2 [%]	T_2 [ps]
(NDI-dH) ₂ PbI ₄	73	0.55 ± 0.04	27	14.3 ± 3.0

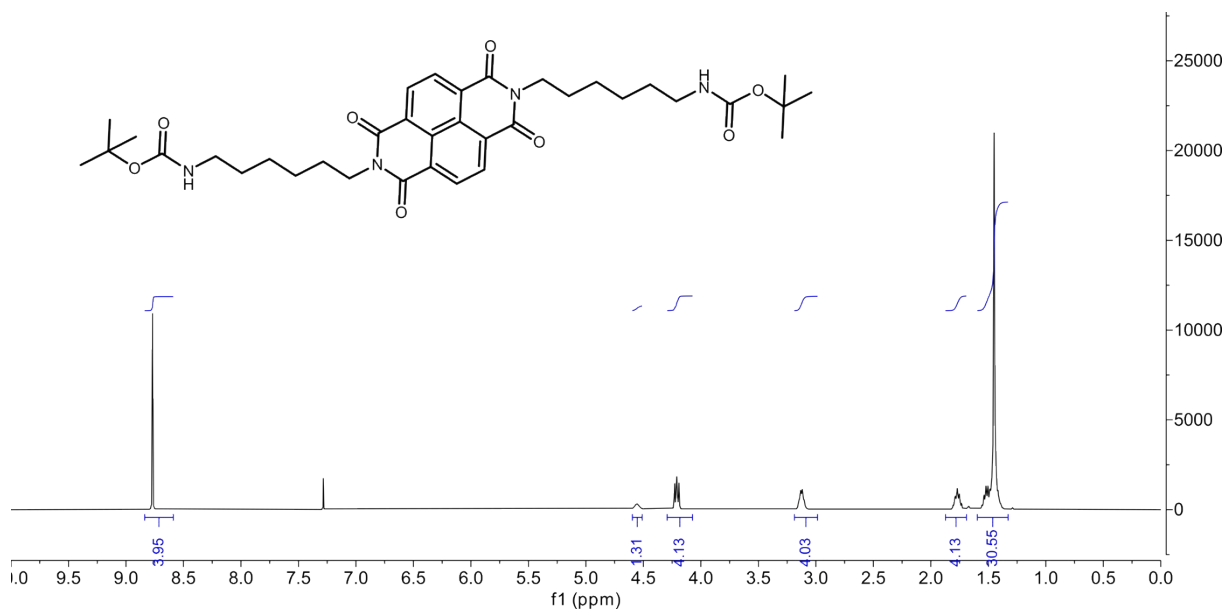
Table S2 Fitted decay time constants for all investigated thin films.

	$n = 1$	$n = 2$	$n = 3$	$\langle n \rangle = 4$	$\langle n \rangle = 5$
τ_1 / ps	1.66	1.83	2.04	2.71	2.56
τ_2 / ps	6.11	58.8	45.3	200	122
T_3 / ps	1510	2450	1609	2380	1540

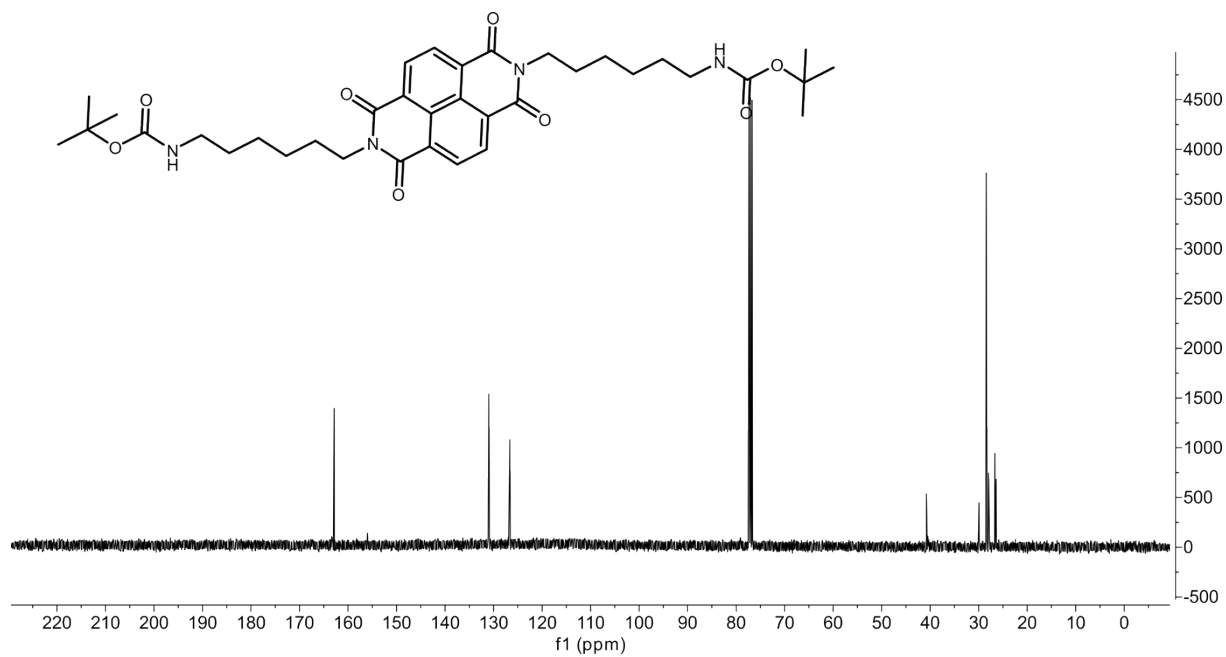
References

- [1] G. C. Fish, J. M. Moreno-Naranjo, A. Billion, D. Kratzert, E. Hack, I. Krossing, F. Nüesch, J.-E. Moser, *Phys. Chem. Chem. Phys.* **2021**, *23*, 23886–23895.
- [2] G. Ashiotis, A. Deschildre, Z. Nawaz, J. P. Wright, D. Karkoulis, F. E. Picca, J. Kieffer, *J. Appl. Crystallogr.* **2015**, *48*, 510–519.
- [3] N. Striebeck, U. Nöchel, *J. Appl. Crystallogr.* **2009**, *42*, 295–301.
- [4] T. J. Savenije, A. J. Ferguson, N. Kopidakis, G. Rumbles, *J. Phys. Chem. C* **2013**, *117*, 24085–24103.
- [5] M. Schleuning, M. Kölbach, F. F. Abdi, K. Schwarzburg, M. Stolterfoht, R. Eichberger, R. van de Krol, D. Friedrich, H. Hempel, *PRX Energy* **2022**, *1*, 023008.
- [6] A. Burgos-Caminal, E. Socie, M. E. F. Bouduban, J.-E. Moser, *J. Phys. Chem. Lett.* **2020**, *11*, 7692–7701.
- [7] M. Saliba, J.-P. Correa-Baena, C. M. Wolff, M. Stolterfoht, N. Phung, S. Albrecht, D. Neher, A. Abate, *Chem. Mater.* **2018**, *30*, 4193–4201.
- [8] K. Yan, M. Long, T. Zhang, Z. Wei, H. Chen, S. Yang, J. Xu, *J. Am. Chem. Soc.* **2015**, *137*, 4460–4468.
- [9] Y. Zhong, M. Hufnagel, M. Thelakkat, C. Li, S. Huettnner, *Adv. Funct. Mater.* **2020**, *30*, 1908920.
- [10] M. D. Murbach, B. Gerwe, N. Dawson-Elli, L. Tsui, *J. Open Source Softw.* **2020**, *5*, 2349.
- [11] M. P. Hughes, K. D. Rosenthal, N. A. Ran, M. Seifrid, G. C. Bazan, T.-Q. Nguyen, *Adv. Funct. Mater.* **2018**, *28*, 1801542.

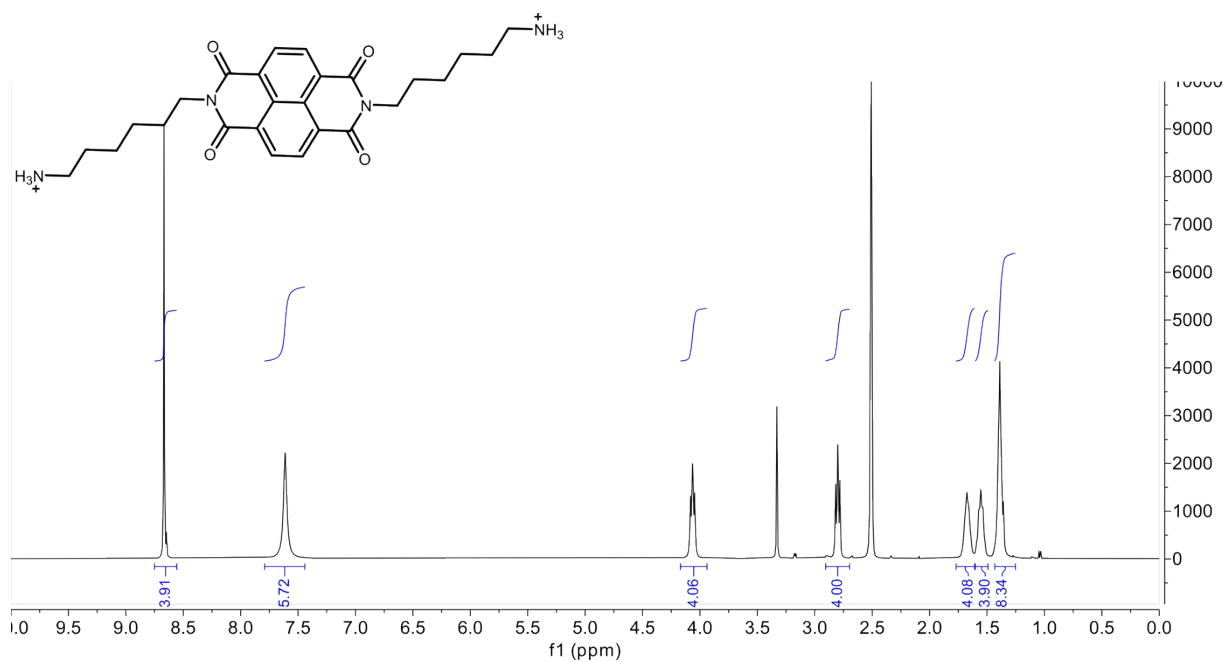
NMR Spectra



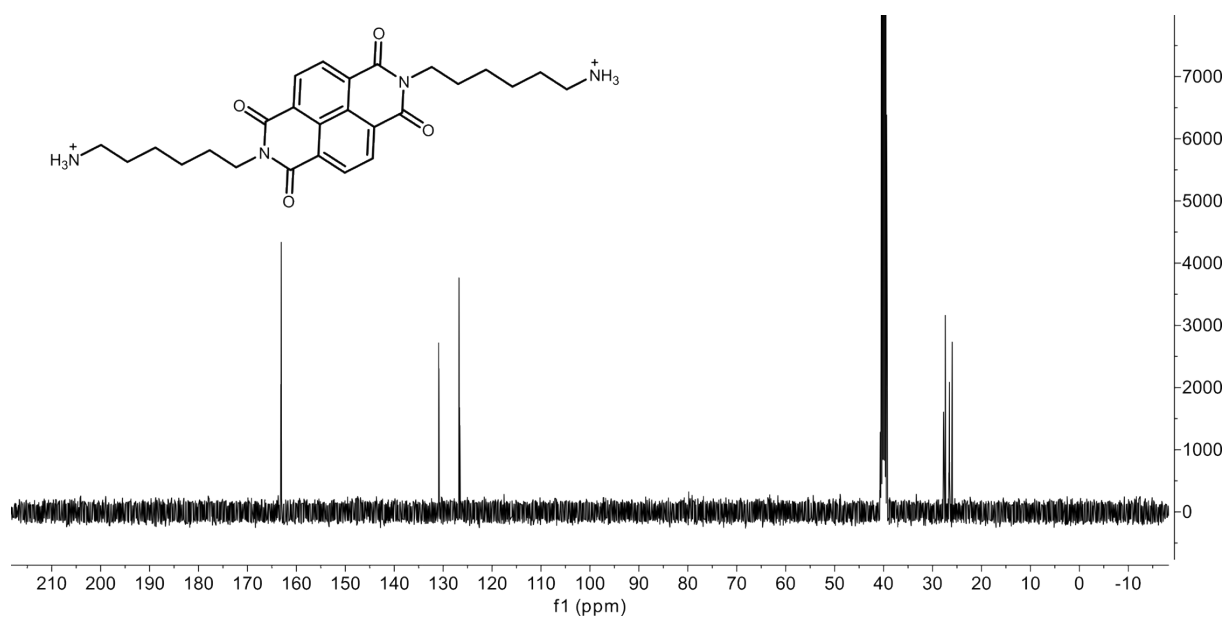
NMR 1: ¹H-NMR of Boc-protected NDI-dH in CDCl₃



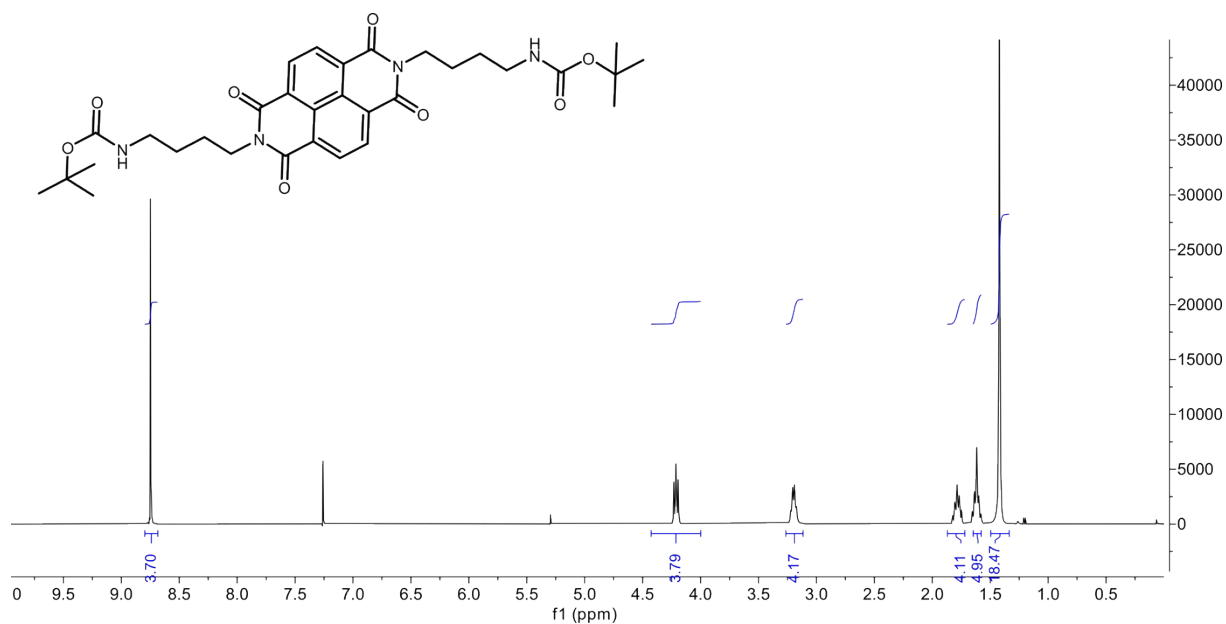
NMR 2: ¹³C-NMR of Boc-protected NDI-dH in CDCl₃



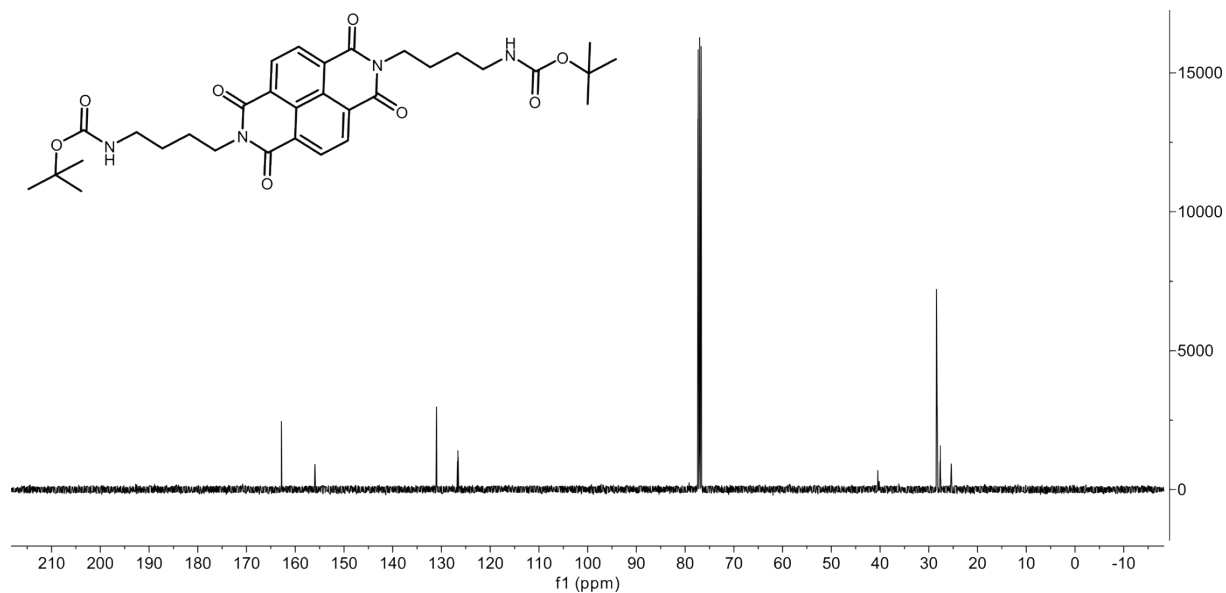
NMR 3: ¹H-NMR of NDI-dH salt in DMSO-d₆



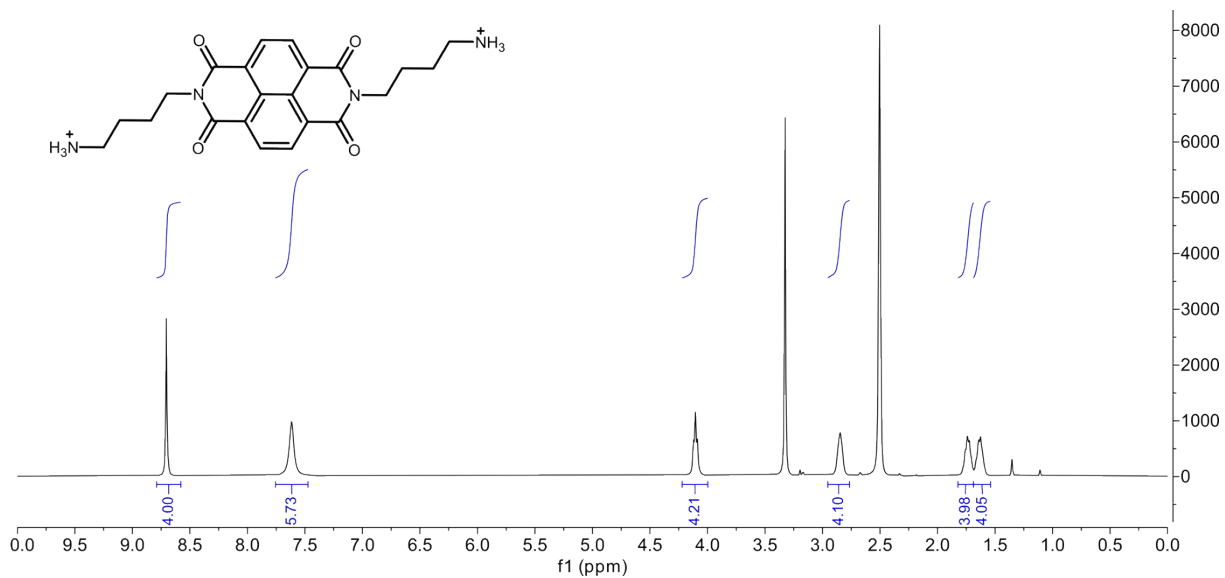
NMR 4: ¹³C-NMR NDI-dH in DMSO-d₆



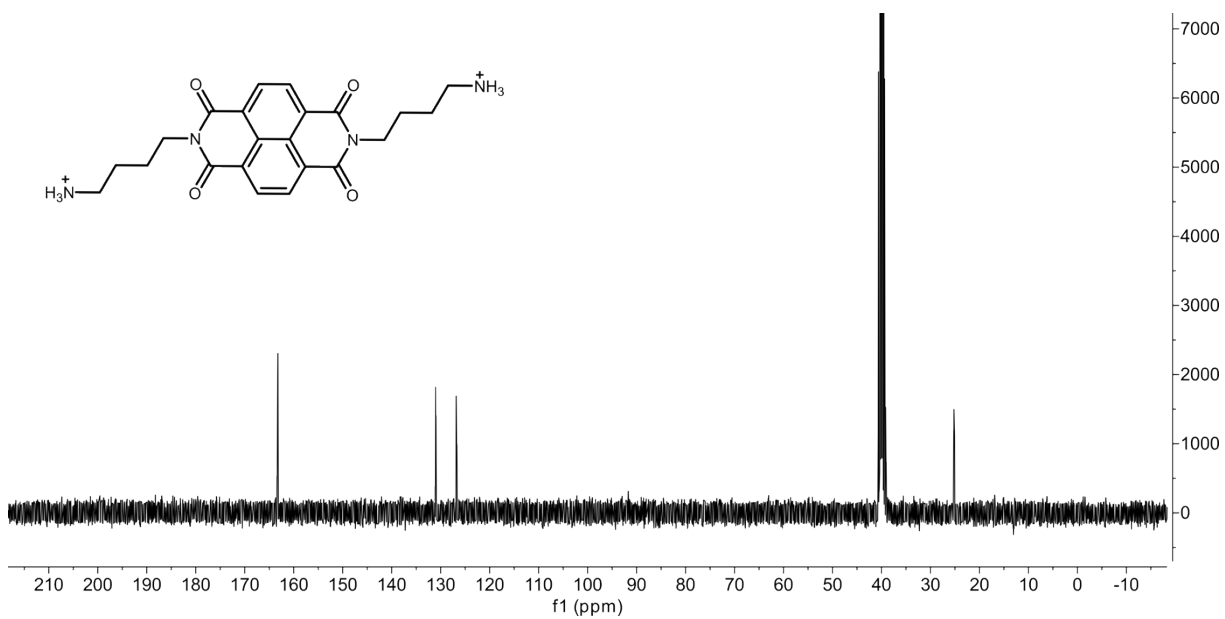
NMR 5: ^1H -NMR of Boc-protected NDI-dB in CDCl_3



NMR 6: ^{13}C -NMR of Boc-protected NDI-dB in CDCl_3



NMR 7: ¹H-NMR of NDI-dB salt in DMSO-d₆



NMR 8: ¹³C-NMR of NDI-dB salt in DMSO-d₆